Nanostructured YbAgCu4 for Potentially Cryogenic Thermoelectric Cooling

ARTICLE *in* NANO LETTERS · JULY 2014

Impact Factor: 13.59 · DOI: 10.1021/nl501436w · Source: PubMed

7 AUTHORS, INCLUDING:

Machhindra Koirala
Boston College, USA
8 PUBLICATIONS **18** CITATIONS
SEE PROFILE

Hui Wang
Newcastle University
162 PUBLICATIONS **2,002** CITATIONS
SEE PROFILE

Mani Pokharel
Boston College, USA
18 PUBLICATIONS **95** CITATIONS
SEE PROFILE

Chuanfei Guo
University of Houston
59 PUBLICATIONS **594** CITATIONS
SEE PROFILE

NANO LETTERS

Letter

pubs.acs.org/NanoLett

Nanostructured $YbAgCu_4$ for Potentially Cryogenic Thermoelectric Cooling

Machhindra Koirala,[†] Hui Wang,[†] Mani Pokharel,[‡] Yucheng Lan,[†] Chuanfei Guo,[†] Cyril Opeil,[‡] and Zhifeng Ren[†,*]

[†]Department of Physics and TcSUH, University of Houston, Houston, Texas 77204, United States

[‡]Department of Physics, Boston College, Chesnut Hill, Massachusetts 02467, United States

ABSTRACT: We have studied the thermoelectric properties of nanostructured $YbAgCu_4$ materials. A high power factor of ~131 μW cm^{-1} K^{-2} has been obtained at 22 K for nanostructured samples prepared by ball milling the arc melted ingot into nanopowder and hot pressing the nanopowder. The implementation of nanostructuring method decreased the thermal conductivity at 42 K by 30−50% through boundary scattering comparing with the previously reported value of polycrystalline $YbAgCu_4$. A peak dimensionless thermoelectric figure-of-merit, ZT, of 0.11 has been achieved at 42 K, which may find potential applications for cryogenic cooling below 77 K. The nanostructuring approach can be extended to other heavy Fermion materials to achieve high power factor and low thermal conductivity and ultimately higher ZT.

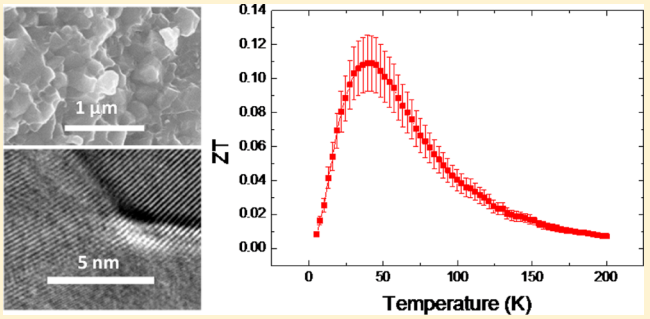

KEYWORDS: *Thermoelectric, heavy Fermions, Kondo lattice, boundary scattering, $YbAgCu_4$*

The ability of thermoelectric (TE) materials for converting heat into electricity and vice versa is very important for power generation[1,2] as well as solid-state cooling.[3] For the aerospace program where the weight and size compatibility of the devices is important, thermoelectric devices are more useful for cryogenic application in comparison to other heavy cooling devices. The power generation efficiency or coefficient of performance of thermoelectric devices are determined by the dimensionless figure of merit, $ZT = [(S^2\sigma)/\kappa]T$, where S is the Seebeck coefficient, σ is the electrical conductivity, κ is the thermal conductivity, and T is the absolute temperature.[4−6] All of these quantities are related to each other and changing one affects the others, so increasing ZT is really challenging. In the recent years, the development of new techniques for controlling the material properties through nanostructuring,[7] modulation doping,[8,9] resonant doping,[10,11] and band engineering near Fermi level[12,13] have helped to enhance ZT significantly. The rapid development of technologies enabled to increases ZT above 1 for cooling applications at around room temperature and power generation at high temperatures but at the low-temperature (cryogenic) range, the existing ZT is far below the application requirement.

For low-temperature thermoelectric materials, most of the focus is toward narrow band gap semiconductors and Kondo insulators. In different temperature ranges below room temperature, there are many materials that are being investigated. The well-known low-temperature thermoelectric material is single crystal $Bi_{1-x}Sb_x$ with ZT ~ 0.5 at ~150 K.[14] Encapsulating Ce in clathrate has enhanced ZT to 0.1 at 150 K.[15] Doping on extremely high mobility materials CuAgSe has enhanced ZT to 0.1 at 100 K.[16] Doped FeSi have been reported to have peak ZT of 0.12 at 120 K.[17] However, the operating temperature for these materials is above 100 K, which is above liquid nitrogen temperature, 77 K. For temperature below 77 K, ZT is very low because the temperature T is very small.

The current trend for cryogenic thermoelectric materials involves mostly Kondo insulators like $FeSb_2$,[18−20] $CrSb_2$,[21] and some rare earth Kondo systems like $YbAl_3$,[22] $CeCu_6$,[23] $Ce_{0.5}La_{0.5}Al_3$,[24] YbCuAl,[25] $CeAl_3$,[25] $CePd_3$,[26] and so forth. Rare earth metallic heavy Fermions like $YbAl_3$, $CePd_3$[26] have been investigated to the temperature range of 150 K and a peak ZT ~ 0.23 have been reported for both n- and p-type. Our focus in this work is to study materials having good ZT at below 77 K. $FeSb_2$ was studied for its giant Seebeck coefficient below 77 K by Bentein.[18] Much effort have been made on that materials but the optimized ZT is not more than 0.026.[18−20,27] In phonon drag systems like $FeSb_2$[28] and $CrSb_2$, it is very difficult to decouple the electrical and phonon part and the value of ZT remains low. There are some rare earth Kondo systems with good power factor at temperature below 77 K, but they have high thermal conductivity so the overall ZT is low. Maintaining that high power factor and reducing thermal conductivity is really challenging.

Received: April 17, 2014
Revised: July 17, 2014
Published: July 31, 2014

   dx.doi.org/10.1021/nl501436w | *Nano Lett.* 2014, 14, 5016−5020

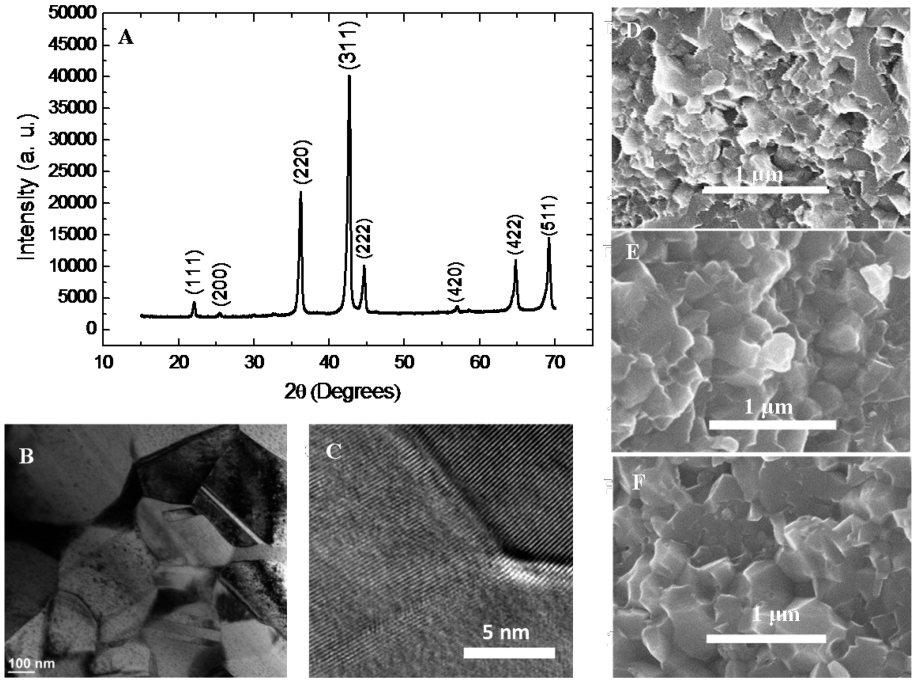

Figure 1. XRD pattern (A) and TEM images (B,C) for $YbAgCu_4$ samples hot pressed at 750 °C, SEM images for $YbAgCu_4$ samples hot pressed at temperatures of 550 (D), 650 (E), and 750 °C (F).

Here, we present the synthesis and characterization of the thermoelectric properties of nanostructured $YbAgCu_4$. This material was discovered as heavy Fermion materials in 1987 by Rossel[29] with moderate effective mass. $YbAgCu_4$ comes from the family of parent compound $YbCu_5$ that is nonmagnetic and metallic with hexagonal structure.[30−32] The replacing of one Cu atom by Ag makes a dramatic change in crystal structure and turns it into face-centered cubic (fcc) structure.[33] The spin exchange interaction between f orbital and conduction electron is much stronger than the intersite Ruderman−Kittel−Kasuya−Yosida (RKKY) interaction and any other possible crystalline field splitting effect.[29,34] There is the presence of the giant Seebeck peak at 45 K which is due to Kondo scattering of conduction electron from almost the full f band.[35] The thermal conductivity of $YbAgCu_4$ is unusually low below 50 K in comparison to other heavy Fermion systems,[36] which makes this material worth for investigation as TE materials. This material has been noted by Mahan[25] as having a high power factor of ∼235 μW cm^{-1} K^{-2} on the basis of two earlier published papers[35,37] by inappropriately using the electrical resistivity data from Graf[37] and Seebeck coefficient data from Casanova.[35] Nevertheless, we endeavor to study the thermoelectric properties of a series of samples to determine whether such a high power factor can be achieved. It is also intended to study whether lower thermal conductivity can be achieved in this material by nanostructuring while maintaining the high power factor.

Experimental Section. Nanostructured $YbAgCu_4$ was prepared by arc melting followed by ball milling process. The stoichiometric ratio of 99.9% pure Ag and 99.9% Cu granular from Alfa Aesar is kept in an arc melting hearth and melted to make the single piece. Pure Yb pieces (99.9%) with 10 % extra form stoichiometric ratio is kept in the arc melting hearth with the Ag−Cu piece and melted together. The main idea for this melting approach is to avoid the direct contact of arc with Yb, which is volatile in nature. The melting process was repeated 8 times by monitoring the total weight loss at each time. The ingot was polished with metal brush and ball milled for 6 h in high energy ball milling machine. The powder was dc hot pressed at 550, 650, and 750 °C and a pressure of 100 MPa for 5 min. The samples were characterized by X-ray diffraction (Panalytical X'pert), high-resolution transmission electron microscope (HRTEM, JEOL 2100F), and scanning electron microscope (SEM, LEO 1525) to characterize the phase formation, crystallinity, homogeneity, grain size distribution, and grain boundary. Samples of 3 × 3 × 5 cm^3 were measured for temperature-dependent electrical conductivity, Seebeck coefficient, and thermal conductivity using thermal transport option by physical properties measurement system (Quantum design, PPMS with TTO).

Results and Discussion. Figure 1A presents the XRD pattern of the sample hot pressed at 750 °C for 5 min. The sample is single phase within the detection limit of the XRD machine and can be indexed by $AuBe_5$-type face-centered cubic structure. The TEM images shown in Figure 1B,C indicate that the grains are closely packed and the crystallinity of the grains is good and the grain boundaries are clean. The samples hot pressed at different temperatures were analyzed using SEM to study the effect of hot pressing temperature on the grain size and distribution. Figure 1D−F shows that the average grain size is 100 ± 25, 175 ± 25, and 225 ± 25 nm for the samples hot pressed at 550, 650, and 750 °C, respectively.

We have measured the thermoelectric properties of $YbAgCu_4$ samples and the results are presented in Figures 2 and 3. Electrical resistivity data are presented in Figures 2A and 3A. It is clearly seen that the samples show pretty strong metallic behavior below 75 K and a weak semiconductor behavior above 75 K. The electrical transport data can be explained in the basis of phenomenological method which is being used for many heavy Fermion systems.[38−40] The dominant contribution to electrical resistivity is due to electron−phonon interaction and scattering of electron between conduction band and

dx.doi.org/10.1021/nl501436w | Nano Lett. 2014, 14, 5016−5020

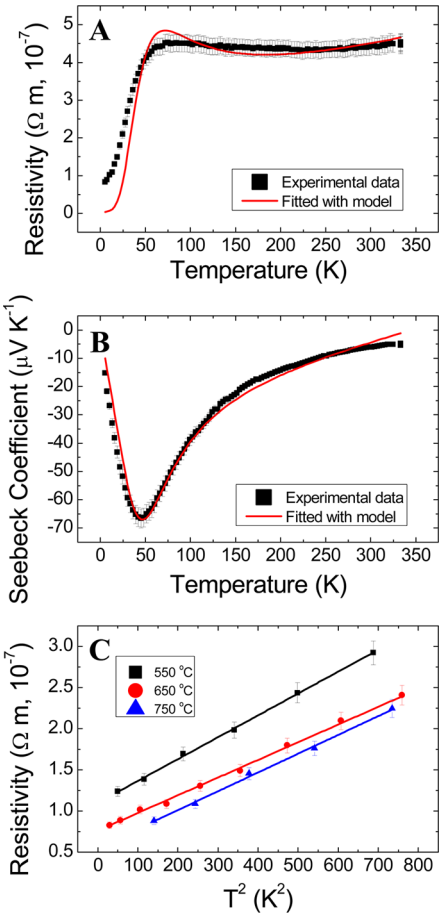

Figure 2. Temperature-dependent resistivity (A) and Seebeck coefficient (B) fitted with phenomenological model for samples hot pressed at 650 °C. Plot of electrical resistivity ρ versus T^2 below 27 K for $YbAgCu_4$ (C).

Lorentzian-shaped 4f band. Using the Mott's analogy, resistivity due to scattering of electron of conduction band and f band is proportional to the density of states of f states at Fermi level.[41] Hence, electrical resistivity can be written as[38,39]

$$\rho = aT + \frac{bW(T)}{(T_o^2 + (W(T))^2)} \quad (1)$$

where $W(T) = T_f \exp(-T_f/T)$ is the width of f band and T_o ($k_\beta T_o = \varepsilon_F - \varepsilon_f$ where ε_F is the Fermi energy and ε_f the is energy corresponding to center of gravity of 4f peak) is the central position of 4f band from Fermi level. The term T_f is a temperature-dependent parameter and related to quasi-elastic line width of neutron spectra. The coefficients a and b represent the strength of electron phonon scattering and the strength of hybridization between s and f bands, respectively. The quasi-elastic line width for $YbAgCu_4$ is reported to be invariant with temperature[42] and the value of T_f is reported to be 100 K.[42,43] The coefficients a and b are obtained from fitting the resistivity curve and found to be 6.51×10^{-10} Ω m K^{-1} and 2.02×10^{-5} Ω m K, respectively. From Figure 2A, we have seen that experimental data can be fitted with model very well with T_o = 23 K. The difference between the experimental and fitted data near the resistivity maxima temperature could be due to defects and the grain boundary presented in the sample.

In the range of 75 to 200 K, there is formation of dilute Kondo system. In that temperature range, there is an increase of electrical resistivity with decreasing temperature. This is due to Kondo scattering of electrons between conduction and f bands. When the temperature goes below 75 K, the dilute Kondo system transformed to Kondo lattice system with sharp decrease in electrical resistivity. Electrical resistivity for samples hot pressed at different temperatures is presented in Figure 3A. The electrical resistivity of a sample hot pressed at 550 °C is higher compared to the other two samples. This can be understood as conduction electron scattering by the weakly linked grain boundary that resulted from the low hot press temperature.

At the very low temperature, the system behaves as Fermi liquid system with resistivity linear to square of the temperature of the system as discussed in refs 33 and 44. At that temperature range, it is not reasonable to expect the matching of experimental data with phenomenological model. Figure 2C shows that the electrical resistivity of all samples can be fitted with Fermi liquid theory below 27 K. The slope of the resistivity with T^2 is proportional to the density of states of conduction electron. In our samples, we have seen that the Fermi liquid behavior can be seen up to 27 K indicating that the electronic motion is not much affected by grain size. Therefore, the nanostructures do not affect the electronic contribution arising from band hybridization of the 4f and conduction bands.

Using the Lorentzian density of states of f band at Fermi level, the Seebeck coefficient can be expressed as

$$S = c_1 T + \frac{c_2 T T_o}{(T_o^2 + (W(T))^2)} \quad (2)$$

where the first term gives the nonmagnetic contribution to Seebeck coefficient and the second term gives the magnetic contribution to Seebeck coefficient. We have used the same value T_f (100 K) and extracted value for T_o (23 K) using resistivity relation and fitted the Seebeck coefficient. Our Seebeck coefficient data match with the phenomenological model with c_1 = 0.175 μV K^{-2} and c_2 = −46.713 μV K^{-1} showing that most of the contribution on the Seebeck coefficient is from the magnetic scattering of conduction electron by the f band. From the extracted value of T_o (23 K), we have found that the center of the f band is 1.9 meV below the Fermi level giving the negative slope of density of states of the f band at Fermi level which makes the negative Seebeck coefficient of $YbAgCu_4$. The presence of a flat f band could enhance the density of states near the Fermi level, which enhances Seebeck coefficient.[45] From Figure 3B, for our nanostructured sample we have achieved absolute maximum Seebeck coefficient of 66 μV K^{-1} at 45 K. From this analysis, we can conclude that the simple phenomenological model can explain Seebeck coefficient of $YbAgCu_4$.

Figure 3C shows the power factor of the $YbAgCu_4$ samples hot pressed at different temperatures. Because the absolute maxima of Seebeck coefficient and resistivity minimum occur at two different temperatures, we observed the highest power factor of 131 μW cm^{-1} K^{-2} at 22 K. Even though it is much lower than 235 μW cm^{-1} K^{-2} calculated by Mahan[25] on the basis of the previously published papers,[35,36] it is already much higher than most of the other good TE materials such as Bi_2Te_3[46] and $Bi_{1-x}Sb_x$.[14] Although very high power factors have been reported for the $FeSb_2$ single crystal,[18] it cannot be maintained in nanostructured samples with very lower thermal conductivity. Thermal conductivity decreases with grain size but also the peak Seebeck coefficient and hence the power

dx.doi.org/10.1021/nl501436w | Nano Lett. 2014, 14, 5016−5020

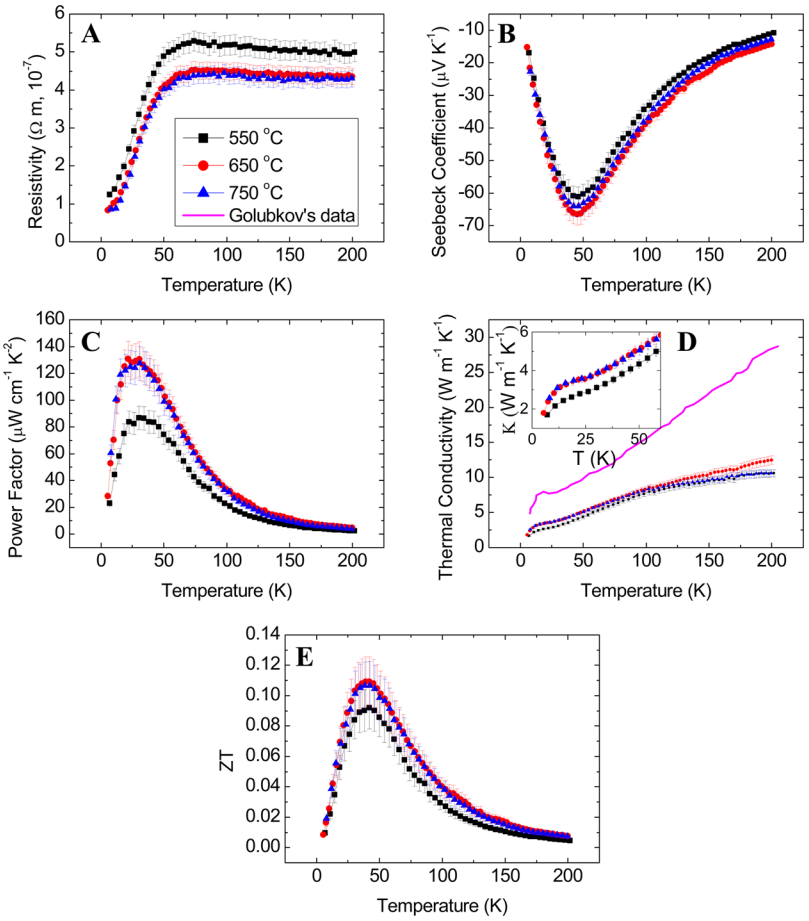

Figure 3. Thermoelectric properties of nanostructured $YbAgCu_4$ samples hot pressed at different temperatures. Temperature-dependent electrical resistivity (A), Seebeck coefficient (B), power factor (C), thermal conductivity with the reference data from Golubkov et al.[36] for comparison (D), and ZT with 15% uncertainty in measurement (E).

factor and overall ZT enhancement is not significant. For our system, we did not notice a big decrease of Seebeck coefficient with grain size. The samples hot pressed at 650 and 750 °C have nearly the same power factors and are higher than that of the sample hot pressed at 550 °C.

Figure 3D shows the thermal conductivity of these samples. They all show a similar trend: decrease with temperature. The thermal conductivity of the samples hot pressed at 550 °C is a little bit smaller than the other two samples hot pressed at a higher temperature. Because the grain size of the samples hot pressed at 650 and 750 °C is not much different, hence the thermal conductivity is also similar. In heavy Fermions systems, the formation of gap due to hybridization of bands enhances the phonon mean free path and hence the thermal conductivity of these materials is very high.[4] In many heavy Fermion systems, the lattice thermal conductivity of doped samples is of the same magnitude of undoped sample[26] suggesting point defect scattering is not effective to decrease thermal conductivity. Short intrinsic electronic mean free path of heavy Fermions suggests that boundary scattering of phonon is one of the promising ways to decrease the thermal conductivity without significantly affecting the electrical properties of such systems.[47] We did not find any report for thermal conductivity of single crystal $YbAgCu_4$ for comparison of boundary scattering. There are a couple of reports on thermal conductivity of polycrystalline $YbAgCu_4$.[36,48] In comparison, the nanostructure reduces the thermal conductivity by 30−50% through boundary scattering of phonons comparing with the earlier reported value for polycrystalline sample (data from ref 36 is plotted in Figure 3D for comparison). Although, the grain size information on the refs 36 and 48 is not available, from their synthesis method it could be speculated that the grain size of their polycrystalline samples should be in the order of several microns.

Figure 3E shows the thermoelectric figure of merit ZT of $YbAgCu_4$ samples. We note a peak ZT of 0.11 at 42 K has been achieved for samples hot pressed at 650 and 750 °C. This is pretty high at this low temperature, which will take us one step further to the cooling applications at this temperature.

In conclusion, we have synthesized and characterized nanostructured $YbAgCu_4$ using ball milling the arc melted ingot and hot pressing method. The Seebeck coefficient in Yb-based heavy Fermions is due to Kondo scattering of electrons between conduction band and 4f band. The electrical resistivity and Seebeck coefficient of nanostructured sample can be explained in terms of the well-known phenomenological model. The good electrical conductivity of $YbAgCu_4$ leads to a high power factor of 131 $\mu W\ cm^{-1}\ K^{-2}$ at 22 K. We have maintained the high power factor with a significantly lower thermal conductivity. The high power factor is clearly advantageous for higher ZT. A peak ZT of 0.11 has been achieved at 42 K, suitable for cooling down to this temperature. Our results bring us one step closer for using TE materials for Peltier cooling purpose below liquid nitrogen temperature. We believe that this

dx.doi.org/10.1021/nl501436w | *Nano Lett.* 2014, 14, 5016−5020

result will attract more research effort for this and other similar material systems to make the TE cooling below liquid nitrogen temperature a reality.

AUTHOR INFORMATION

Corresponding Author

*E-mail: zren@uh.edu.

Notes

The authors declare no competing financial interest.

ACKNOWLEDGMENTS

The work was financially supported by Air Force Office of Scientific Research's MURI program under Contract No. FA9550-10-1-0533.

REFERENCES

(1) Ioffe, A. F. *Physics of Semiconductors*; Academic Press: New York, 1960.
(2) Slack, G. A.; Hussain, M. A. *J. Appl. Phys.* **1991**, *70*, 2694.
(3) Taylog, R. A.; Solbrekken, G. L. *IEEE Trans. Compon. Packag. Technol.* **2008**, *31*, 23.
(4) Rowe, D. M. *CRC Handbook of Thermoelectrics*; CRC Press: Boca Raton, 1995.
(5) Goldsmid, H. J *Thermoelectric Refrigeration*; Plenum: New York, 1964.
(6) Tritt, T. M. *Semiconductor and Semimetals, Recent Trends in Thermoelectric Materials Research, Part 1−3*; Academic: San Diego, CA, 2001; Vol. *69−71*.
(7) Poudel, B.; Hao, Q.; Ma, Y. C.; Lan, Y.; Minnich, A.; Yu, B.; Yan, X.; Wang, D. Z.; Muto, A.; Vashaee, D.; Chen, X.; Liu, J.; Dresselhaus, M. S.; Chen, G.; Ren, Z. F. *Science* **2008**, *320*, 634.
(8) Zebarjadi, M.; Joshi, G.; Zhu, G.; Yu, B.; Minnich, A.; Lan, Y. C.; Wang, X.; Dresselhaus, M.; Ren, Z. F.; Chen, G. *Nano Lett.* **2011**, *11*, 2225.
(9) Yu, B.; Zerbarjadi, M.; Wang, H.; Lukas, K.; Wang, H.; Wang, D.; Opeil, C.; Dresselhaus, M.; Chen, G.; Ren, Z. F. *Nano Lett.* **2012**, *12*, 2077.
(10) Heremans, J. P.; Jovovic, V.; Toberer, E. S.; Saramat, A.; Kurosaki, K.; Charoenphakdee, A.; Yamanaka, S.; Snyder, G. J. *Science* **2008**, *321*, 554.
(11) Heremans, J. P.; Wiendlocha, B.; Chamoire, A. M. *Energy Environ. Sci.* **2012**, *5*, 5510.
(12) Pei, Y. Z.; Shi, X. Y.; LaLonde, A.; Wang, H.; Chen, L. D.; Snyder, G. J. *Nature* **2011**, *473*, 66.
(13) Zhang, Q.; Cao, F.; Liu, W. S.; Lukas, K.; Yu, B.; Chen, S.; Opeil, C.; Broido, D.; Chen, G.; Ren, Z. F. *J. Am. Chem. Soc.* **2012**, *134*, 10031.
(14) Smith, G. E.; Wolfe, R. *J. Appl. Phys.* **1962**, *33*, 841.
(15) Prokofiev, A.; Sidorenko, A.; Hradil, K.; Ikeda, M.; Svagera, R.; Waas, M.; Winkler, H.; Neumaier, K.; Paschen, S. *Nat. Mater.* **2013**, *12*, 1096.
(16) Ishiwata, S.; Shiomi, Y.; Lee, J. S.; Bahramy, M. S.; Suzuki, T.; Uchida, M.; Arita, R.; Taguchi, Y.; Tokura, Y. *Nat. Mater.* **2013**, *12*, 512.
(17) Sales, B. C.; Delaire, O.; McGuire, V. L.; May, A. F. *Phys. Rev. B* **2011**, *83*, 125209.
(18) Bentien, A.; Johnson, S.; Madsen, G. K. H.; Iverson, B. B.; Steglich, F. *Europhys. Lett.* **2007**, *80*, 17008.
(19) Zhao, H. Z.; Pokharel, M.; Zhu, G.; Chen, S.; Lukas, K.; Jie, Q.; Opeil, C.; Chen, G.; Ren, Z. F. *Appl. Phys. Lett.* **2011**, *99*, 163101.
(20) Koirala, M.; Zhao, H. Z.; Pokharel, M.; Chen, S.; Dahal, T.; Opeil, C.; Chen, G.; Ren, Z. F. *Appl. Phys. Lett.* **2013**, *102*, 213111.
(21) Sales, B. C.; May, A. F.; McGuire, M. A.; Stone, M. B.; Singh, D. J.; Mandrus, D. *Phys. Rev. B* **2012**, *86*, 235136.
(22) Lehr, G. J.; Morelli, D. T. *J. Electron. Mater.* **2013**, *42*, 1697.
(23) Ocko, M.; Miljak, M.; Kost, I.; Park, J.-G.; Roy, S. B. *J. Phys.: Condens. Matter* **1995**, *7*, 2979.
(24) Van Aken, P. B.; Van Daal, H. J.; Buschow, K. H. J. *Phys. Lett. A* **1974**, *49*, 201.
(25) Mahan, G. D. *Solid State Physics* **1998**, *51*, 81.
(26) Mahan, G. D.; Sales, B.; Sharp, J. *Phys. Today* **1997**, *50* (3), 42.
(27) Sun, P.; Sondergaard, M.; Sun, Y.; Johnsen, S.; Iversen, B. B.; Steglich, F. *Appl. Phys. Lett.* **2011**, *98*, 072105.
(28) Pokharel, M.; Zhao, H.; Lukas, K.; Ren, Z. F.; Opeil, C.; Mihaila, B. *MRS Commun.* **2013**, *3*, 31.
(29) Rossel, C.; Yang, K. N.; Maple, M. B.; Fisk, Z.; Zirngiebl, E.; Thompson, J. D. *Phys. Rev. B* **1987**, *35*, 1914.
(30) Tsujii, N.; He, J.; Amita, F.; Yoshimura, K.; Kosuge, K.; Michor, H.; Hilscher, G.; Goto, T. *Phys. Rev. B* **1997**, *56*, 8103.
(31) Mitsuda, A.; Yamauchi, K.; Tsujii, N.; Yoshimura, K.; Isikawa, Y.; Yamada, Y. *J. Phys. Soc. Jpn.* **2007**, *76*, 78.
(32) Yamaoka, H.; jarrige, I.; Tsujii, N.; Hiraoka, N.; Ishii, H.; Tuesi, K.-D. *Phys. Rev. B* **2009**, *80*, 035120.
(33) Tsujii, N.; He, J.; Yoshimura, K.; Kosuge, K.; Michor, H.; Kreiner, K.; Hilscher, G. *Phys. Rev. B* **1997**, *55*, 1032.
(34) Schlottmann, P. *J. Appl. Phys.* **1993**, *73*, 5412.
(35) Casanova, R.; Jaccard, D.; Marcenat, C.; Hamdaoui, C.; Besnus, M. J. *J. Magn. Magn. Mater.* **1990**, *90 & 91*, 587.
(36) Golubkov, A. V.; Parfen'eva, L. S.; Smirnov, I. A.; Misiorek, H.; Mucha, J.; Jezowski, A. *Phys. Solid State* **2001**, *43*, 218.
(37) Graf, T.; Lawrence, J. M.; Hundley, M. F.; Thompson, J. D.; Lacerda, A.; Haanappel, E.; Torikachvili, M. S.; Fisk, Z.; Canfield, P. C. *Phys. Rev. B* **1995**, *51*, 15053.
(38) Freimuth, A. *J. Magn. Magn. Mater.* **1987**, *68*, 28.
(39) Grade, C. S.; Ray, J. *Phys. Rev. B* **1995**, *51*, 2960.
(40) Gumeniuk, R.; Sarkar, R.; Geibel, C.; Schnelle, W.; Paulmann, C.; Beanitz, M.; Tsirlin, A. A.; Guritanu, V.; Sichelschmidt, J.; Grin, Y.; Leithe-Jasper, A. *Phys. Rev. B* **2012**, *86*, 235138.
(41) Mott, N. F. *Proc. Phys. Soc.* **1935**, *47*, 571.
(42) Severing, A.; Murani, A. P.; Thompson, J. D.; Fisk, Z.; Loong, C.- K. *Phys. Rev. B* **1990**, *41*, 1739.
(43) Luthi, B. *Physical Acoustics in the Solid State*; Springer Series in Solid-State Sciences; Springer-Verlag, Berlin Heidelberg, 2005; p 148.
(44) Bauer, E.; Hausser, R.; Gratz, E.; Payer, K. *Phys. Rev. B* **1993**, *48*, 15873.
(45) Sun, P.; Ikeno, T.; Mizushima, T.; Isikawa, Y. *Phys. Rev. B* **2009**, *80*, 193105.
(46) Goncalves, L. M.; Couto, C.; Alpuimb, P.; Rolo, A. G.; Völkleinc, F.; Correia, J. H. *Thin Solid Films* **2009**, *518*, 2816.
(47) Zhang, Y.; Dresselhaus, M.; Shi, Y.; Ren, Z. F.; Chen, G. *Nano Lett.* **2011**, *11*, 1166.
(48) Bauer, E.; Gratz, E.; Hutflesz, G.; Bhattacharjee, A. K.; Coqblin, B. *Phys. B* **1993**, *186 − 188*, 494.